

See discussions, stats, and author profiles for this publication at: <https://www.researchgate.net/publication/281419268>

Model for the Evolution of Pore Structure in a Lignite Particle during Pyrolysis

ARTICLE *in* ENERGY & FUELS · JULY 2015

Impact Factor: 2.79 · DOI: 10.1021/acs.energyfuels.5b00726

READS

52

4 AUTHORS, INCLUDING:



Sufen Li

Dalian University of Technology

18 PUBLICATIONS 52 CITATIONS

[SEE PROFILE](#)



He Yang

Dalian University of Technology

5 PUBLICATIONS 14 CITATIONS

[SEE PROFILE](#)



Thomas H. Fletcher

Brigham Young University - Provo Main Campus

155 PUBLICATIONS 2,299 CITATIONS

[SEE PROFILE](#)

Model for the Evolution of Pore Structure in a Lignite Particle during Pyrolysis

Sufen Li,^{*,†} He Yang,[†] Thomas H. Fletcher,[‡] and Ming Dong[†]

[†]School of Energy and Power Engineering, Dalian University of Technology, Dalian 116024, China

[‡]Chemical Engineering Department, Brigham Young University, Provo, Utah 84602, United States

ABSTRACT: In this paper, on the basis of the chemical percolation devolatilization (CPD) model and using the coal polymer network parameters to calculate the surface area and porosity of the particle, a model for the evolution of pore structure in a lignite particle during pyrolysis is established. The model connects the polymer network structure and the pore structure, and it may extend the application range of network statistical devolatilization models. Model predictions agree with experimentally observed trends reported in the literature for porosity and internal surface area with increasing mass release. Particle porosity increases during pyrolysis because of mass release and the opening of closed pores. Surface area changes little with mass release up to about 30% and then increases by 200 m²/g with further increases in mass release; this tendency is determined by the quantity of the pores that can adsorb adsorbent in the particle during pyrolysis. During the pyrolysis of Zap lignite, with the mass release increasing up to 30%, the quantity of pores that can adsorb adsorbent increases from 0 to 0.2 per aromatic cluster, and with the mass release increasing from 30 to 67%, the quantity of pores that can adsorb adsorbent increases from 0.2 to 1.2 per aromatic cluster. With the maximum particle temperature increasing from 900 to 1200 K, it is observed that the predicted porosity of char formed from Zap lignite during pyrolysis increases from 40.1 to 55.3%, the N₂ surface area increases from 18 to 447 m²/g, and the CO₂ surface area increases from 261 to 909 m²/g. However, with further increase of the maximum particle temperature, the predicted porosity and area change little. The influence of heating rate and ambient pressure on the change of pore structure during pyrolysis is small. The initial coal polymer structure significantly influences the final pore structure of the char.

1. INTRODUCTION

During pyrolysis, the porosity, surface area, and density of the coal particle change significantly, which in turn influence the heterogeneous reaction rate of the char and formation of ash.^{1–4} Therefore, the description of the evolution of the pore structure during devolatilization is essential to modeling coal combustion.

The change of lignite pore structure during pyrolysis is different from other kinds of coals. During devolatilization of most coals, particles become plastic and swell, and the swelling can be described by bubble models.^{5–8} However, because the content of metaplast in the particle of lignite during pyrolysis is small, the diameter of lignite changes little during pyrolysis with no thermoplastic deformation,⁹ and some kinds of lignites are classified as nonswelling coals. The porosity of lignite particle increases with increasing mass release during pyrolysis,^{10,11} and this tendency is the same for high-volatile bituminous coals. Little changes of the N₂ surface areas of bituminous coal and subbituminous coal during pyrolysis are observed in experiments.⁹ However, although the N₂ surface areas of lignite also change little with mass release up to about 30%, the N₂ surface area increases from about 5 m²/g to more than 200 m²/g with mass release increasing from 30 to 60%.⁹ The CO₂ surface area of bituminous coal decreases and then increases with mass release increasing from 0 to 30%, whereas the CO₂ surface area of lignite changes little in this mass release region. CO₂ surface areas of bituminous coal and lignite both increase from 200 to 400 m²/g with mass release increasing from 30 to 60%.^{11,12} The porosity of char particles generated from high-volatile

bituminous coal increases and then decreases with increasing maximum particle temperature (T_{\max}) and heating rate.¹³ The porosity of char particles generated from lignite increases with increasing T_{\max} .^{14,15} At particle temperatures higher than 1500 K, porosity increases with increasing T_{\max} rapidly. Gale et al.¹¹ observed that the porosity of char particle generated from Beulah Zap lignite was 54% at a T_{\max} of 1350 K, but at a T_{\max} of 1650 K, the porosity was 66%. The surface area of char particles generated from lignite increases with increasing T_{\max} .^{14–17} However, at very high temperatures, the surface area of some kinds of lignite decreases with increases in temperature.^{18,19} The rapid increase of porosity and decrease of surface area with increasing T_{\max} at very high temperatures may be caused by metaplast and melted ash. Although the particle diameter changes little during pyrolysis, at very high heating rates and temperatures the lignite can also be observed to have melted, bubbled, and swollen.²¹

Few models have been developed to describe pore expansion in a nonswelling coal particle during pyrolysis or in a swelling coal particle during the solid stage of pyrolysis. Previous simulations of the pressure evolution in a lignite particle during pyrolysis have assumed that the inner surface area is constant and that porosity has a linear relationship with mass release.^{20,21} However, as described in above, the pore structure does not change linearly with mass release. A more realistic model for

Received: April 6, 2015

Revised: July 23, 2015

Published: July 26, 2015



the evolution of pore structure in a lignite particle during pyrolysis is therefore needed.

Coal may be viewed as a polymer network consisting of aromatic clusters with aliphatic bridges, loops, and side chains.²² The change of pore structure in a lignite particle during pyrolysis is caused by the changing structure of the network and the changing amount of the aromatic clusters and their aliphatic attachments with volatile generation, and the expansion of pores is caused by increasing voids as the volatiles leave the particle. Therefore, it seems logical that the pore structure can be described by the coal polymer network structure parameters. ¹³C-nuclear magnetic resonance (NMR) structural parameters (p , fraction of attachments that are intact loops or bridges; c , fraction of the charred bridges; $\sigma+1$, coordination number, average number of attachments per aromatic cluster; M_{clust} , average aromatic cluster molecular weight, including associated attachments; and M_{δ} , average molecular weight of a side chain) can be used to determine the compositions of various chemical moieties within coals. Network statistical devolatilization models have been used widely to describe the pyrolysis reaction.^{23–25} These include the functional-group-depolymerization, vaporization, and cross-linking (FG-DVC) model,^{26,27} the FLASHCHAIN model,^{28–30} and the chemical percolation devolatilization (CPD) model.^{9,31,32}

In this paper, using the parameters in the CPD model (the population of intact bridges, population of side chains, and volatile yield) to calculate the particle surface area and porosity, a model for the evolution of pore structure in a lignite particle during pyrolysis is presented. This model connects the polymer network structure parameters in the CPD model to the pore structure, and it may extend the application range of network statistical devolatilization models. The calculation results of the model are compared with experimental results to evaluate the model, and the influences of heating conditions and coal polymer structure parameters on the change of pore structure during pyrolysis are analyzed.

2. MODELING

2.1. CPD Model. In this paper, the pyrolysis reaction is described by the CPD model.^{31–33} The CPD model includes (a) a description of the chemical structure of the parent coal, (b) a kinetic scheme for breaking labile bonds and side chains, (c) percolation statistics based on a Bethe lattice for freeing molecules from the coal particle, (d) a vapor–liquid equilibrium treatment of metaplast versus tar, and (e) a cross-linking mechanism for reattaching metaplast to the solid char.

In the CPD model, coal is defined as a macromolecular array, the building blocks of which are clusters of fused aromatic rings of various sizes and types. These aromatic clusters are interconnected by a variety of chemical bridges, some of which are labile bonds that break readily during coal pyrolysis, whereas others are stable at a given temperature. The bridges that remain intact throughout a given thermal process are referred to as char bridges. A labile bridge decomposes to form a reactive bridge intermediate, which is unstable and quickly reactive in one of two competitive reactions. In one reaction pathway, the reactive intermediate bridge is cleaved, and the two halves form side chains δ that remain attached to the aromatic cluster. The side chains eventually undergo a cracking reaction to form light gas g_1 . In a second, competing reaction pathway, the reactive intermediate is stabilized to form a stable

char bridge c with the associated release of light gas g_2 . When all the bridges connected to an aromatic cluster are cleaved, this cluster is completely detached from the infinite lattice network, and after vaporization, it forms tar.

2.2. Pore Structure Model Developed in This Paper.

The time-dependent value of coal polymer network parameters and volatile yield during pyrolysis can be calculated by CPD model. On the basis of the changes of these parameters, changes in the particle surface area and porosity during pyrolysis are calculated.

2.2.1. Assumptions.

- (1) The coal particle is a porous media, and the diameter is constant with no fragmentation or thermoplastic deformation during pyrolysis.
- (2) The coal particle is spherical and isotropic, and the pores are distributed uniformly in the particle.

The rationale for these assumptions has been discussed in previous study about lignite.²¹

2.2.2. Porosity. Pores in coal particles can be classified into open pores (connecting with outside) and closed pores (not connecting with outside). In experiments, only the open pores can be measured, and the porosity in this paper refers to the open pore porosity.

The closed pores are enclosed by aromatic clusters and bridges. When the bridges cleave, the closed pores are opened and become part of open pores. It is assumed that the quantity of opened pores has a linear relationship with cleaved bridges. The enlargement of the porosity caused by opening of the closed pores is described by eq 1

$$\theta_{\text{OCP}} = f_{\text{PC}}^0 (1 - \theta_0)(1 - p/p_0) \quad (1)$$

where f_{PC}^0 represents the initial volume fraction of closed pores in the solid in the particle, θ_0 represents the initial porosity of the coal particle, and p and p_0 represent the fraction of intact bridges and its initial value, respectively.

With volatile generation, the voids in the coal macromolecular array left as gas and tar molecules are released. These voids become new pores, which in turn enlarge the particle porosity. It is assumed that the solid density (on a pore-free basis) remains constant. The porosity expansion caused by generation of gas and tar are described by eqs 2 and 3, respectively:

$$\theta_{\text{gas}} = f_{\text{gas}} (1 - \theta_0)(1 - f_{\text{PC}}^0)(1 - A_{\text{dry}}) \quad (2)$$

$$\theta_{\text{tar}} = f_{\text{tar}} (1 - \theta_0)(1 - f_{\text{PC}}^0)(1 - A_{\text{dry}}) \quad (3)$$

where f_{gas} and f_{tar} represent the yield of gas and tar on a dry ash-free basis, respectively, and A_{dry} represents ash content of a dry basis.

The total porosity θ therefore consists of θ_{OCP} , θ_{gas} , and θ_{tar} . Equations 1–3 are combined as shown in eq 4.

$$\theta = \theta_0 + (1 - \theta_0)[(f_{\text{tar}} + f_{\text{gas}})(1 - f_{\text{PC}}^0)(1 - A_{\text{dry}}) + f_{\text{PC}}^0 (1 - p/p_0)] \quad (4)$$

2.2.3. Surface Area. The surface area of the particle can be estimated by the quantity of the adsorbate (N_2 or CO_2) molecules in a monolayer molecular adsorption in the coal particle, as shown in eq 5.

$$S_{\text{particle}} = S_a N_A n_a \quad (5)$$

where S_a represents the adsorption cross section of the adsorbing species, N_A represents Avogadro's number, and n_a represents the moles of adsorbate molecules.

With the generation of volatiles (g_1 , g_2 , and tar) during pyrolysis, the solid positions in the coal macromolecular array originally occupied by volatile molecules are emptied to transform into part of the pores in the particle.

However, not all the spaces left by volatiles can increase the surface area, and only the spaces on the surface of solid that are big enough for adsorbates to come in can be measured in the monolayer molecular adsorption.

Each space left by g_2 in the particle (g_2 space) is filled by a char bridge and is not big enough to adsorb one adsorbate molecule.

The light gas molecule size is close to that of an adsorbate molecule so that the size of the space left by g_1 in the particle (g_1 space) should be close to that of an adsorbate molecule, and in this work it is assumed that when both of two interfacing chains are transformed to g_1 the pore consisting of the two g_1 spaces is big enough for one adsorbent molecule to move in. The fraction of this kind of pores in g_1 spaces is estimated as follows:

$$f_{g_1 \text{ space}}^{\text{adsorption pore}} = g_1 / (\delta + g_1) \quad (6)$$

Each aromatic cluster can be regarded as surrounded by the intact bridges (including char bridges) and g_1 spaces. The quantity of g_1 spaces attached to each aromatic cluster is described in eq 7.

$$N_{\text{cluster}}^{g_1 \text{ space}} = \frac{g_1}{2}(\sigma + 1) \quad (7)$$

The quantity of pores consisting of two g_1 spaces that can adsorb adsorbent, per aromatic cluster, is calculated as follows:

$$N_{\text{cluster}}^{\text{adsorption pore}} = \frac{g_1^2(\sigma + 1)}{4(\delta + g_1)} \quad (8)$$

A tar molecule can only be generated after all the bridges connected to an aromatic cluster are cleaved. The surface area generated by tar leaving was already accounted for by the change in g_1 spaces between tar spaces and the solid surface and therefore not accounted for separately. However, with generation of tar, some g_1 spaces attached to the aromatic clusters will be removed from the particle and the particle surface area will decrease.

The quantity of the aromatic clusters in the particle is described in eq 9

$$N_{\text{clust-coal}} = (1 - A_{\text{dry}}) \left(\frac{1}{M_{\text{clust}}} - N_{\text{clust-tar}} \right) m_p^0 \quad (9)$$

where $1/M_{\text{clust}}$ represents the initial population of clusters per mass of dry ash-free coal, $N_{\text{clust-tar}}$ represents the population of clusters removed out of the particle by evaporation of tar per mass of dry ash-free coal, and m_p^0 represents the initial mass of the dry coal particle.

It is assumed that the surface area of the ash in coal does not change during pyrolysis. The balance of the initial surface area of the coal particle during pyrolysis is described in eq 10

$$S_{\text{particle}}^{t_0} = s_{\text{particle}}^0 [(N_{\text{clust-coal}} M_{\text{clust}}) + A_{\text{dry}}] m_p^0 \quad (10)$$

where s_{particle}^0 represents the initial specific surface area of the coal particle.

The final specific surface area is described by eq 11.

$$s_{\text{particle}} = \frac{S_a N_A N_{\text{cluster}}^{\text{adsorption pore}} N_{\text{clust-coal}} + s_{\text{particle}}^{t_0}}{(1 - f_{\text{tar}} - f_{\text{gas}})/(1 - A_{\text{dry}}) + A_{\text{dry}}} \quad (11)$$

2.3. Calculation Conditions. Beulah Zap lignite (75–106 μm), Glen Harold Mine lignite (53–212 μm), and Savage Mine lignite (53–75 μm) are selected to verify the accuracy of the model. The ultimate and proximate analysis of these coals reported in the literature^{9,12} are shown in Table 1.

Table 1. Coal Parameters

Coal	C _{daf} (%)	H _{daf} (%)	N _{daf} (%)	O _{daf} (%)	V _{daf} (%)	A _{dry} (%)
Beulah Zap ⁹	66.6	4.3	1.1	25.2	46.6	18.7
Glen Harold Mine ¹²	71.0	4.9	1.6	21.9	47.5	9.7
Savage Mine ¹²	71.6	4.9	0.8	22.4	43.5	9.5

The chemical structure parameters of the parent coal were calculated from a correlation³⁴ developed for use with the CPD model as shown in Table 2.

Table 2. Chemical Structure Parameters of the Parent Coal

Coal	p ₀	c ₀	M _{clust} (g/mol)	M _δ (g/mol)	σ+1
Beulah Zap	0.67	0.15	352.3	52.6	4.4
Glen Harold Mine	0.60	0.13	342.3	44.7	4.8
Savage Mine	0.62	0.14	338.8	43.4	4.9

The pyrolysis conditions for the calculations are shown in Table 3.

Table 3. Pyrolysis Conditions^a

Coal	θ ₀ (%)	$\frac{s_{\text{particle}}^0 (\text{m}^2/\text{g})}{N_2}$	T _{max} (K)	Ṫ (K/s)
Beulah Zap	13	5	200	3.75×10^4
Glen Harold Mine	16	5	187	1.00×10^4
Savage Mine	8	5	218	1.00×10^4

^aT_{max} is the maximum particle temperature; Ṫ is the heating rate.

In addition, the changes of porosity and surface area of lignite during pyrolysis at various maximum particle temperatures, heating rates, and ambient pressures are calculated to analyze the effects of heating conditions on the change of lignite pore structure during pyrolysis. On the basis of the assumption that there is no fragmentation or thermoplastic deformation during pyrolysis, through comparing the changes of porosity and surface area during pyrolysis of coals with changing polymer network structure parameters at the same heating condition, the effect of each coal parameter on the final char pore structure during pyrolysis is analyzed.

3. RESULTS AND DISCUSSION

The maximum particle temperature, heating rate, and pressure influence the final volatile yield and the pore structure of char, and these influences will be discussed in sections 3.3–3.5, respectively. However, the predicted pore structure parameters at the same mass release change little with the heating

conditions. The predicted change of pore structure parameters with increasing mass release by the model in this paper are compared with three sets of experimental data^{9,11,12} to verify the model and describe the mechanism of pore expansion during pyrolysis in sections 3.1 and 3.2. The experimental data were obtained at particle heating rates from 8.0×10^3 to 7.47×10^4 K/s and T_{\max} from 972 to 1625 K, and the predictions are made on the basis of the conditions in Table 3. In addition, the influence of coal polymer structure parameters is analyzed in section 3.6.

3.1. Change of Porosity during Pyrolysis. The porosity of lignite calculated by the model in this paper compares well with the experimental data,^{9,11,12} as shown in Figure 1.

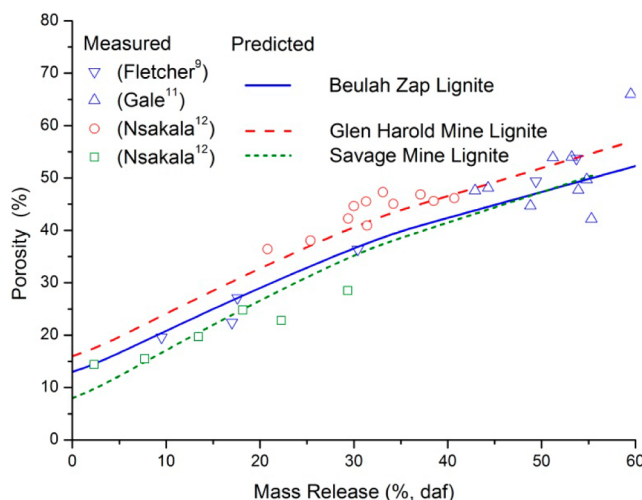


Figure 1. Comparison of the predicted and measured porosity of lignite coal particles.

The evolution of θ , θ_{OCP} , θ_{gas} , and θ_{tar} of Zap lignite during pyrolysis at a heating rate of 3.75×10^4 K/s, T_{\max} of 1250 K, and ambient pressure of 0.1 MPa is shown in Figure 2.

At the beginning of pyrolysis, with the bridges cleaved, the closed pores are opened and g_1 , g_2 , and tar are generated together, which in turn increases θ_{OCP} , θ_{gas} , and θ_{tar} making the particle porosity increase rapidly with increasing mass release.

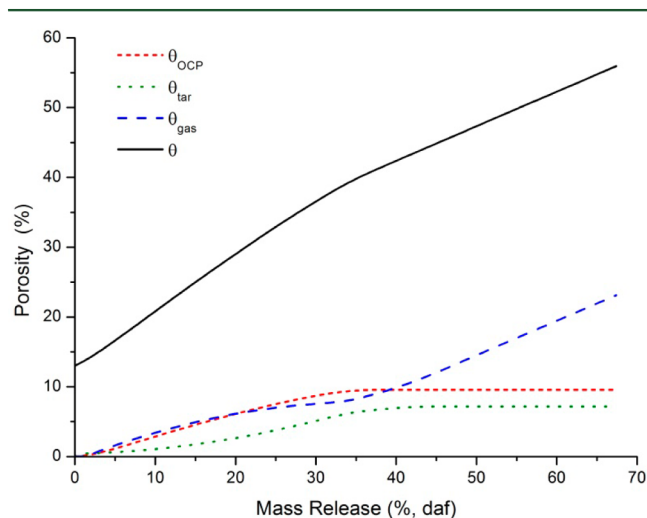
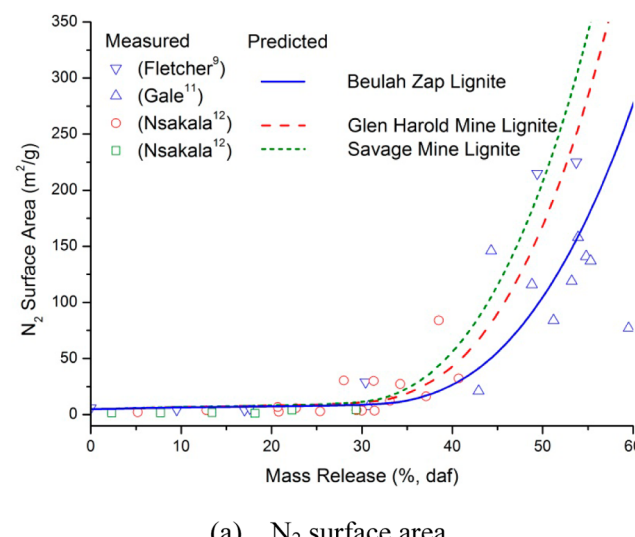


Figure 2. Evolution of predicted θ , θ_{OCP} , θ_{gas} , and θ_{tar} with mass release (Zap lignite).

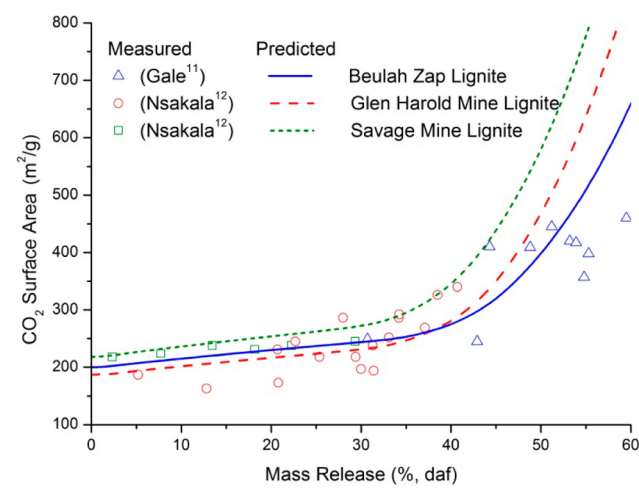
When the mass release is greater than 30%, because most of the labile bridges are cleaved, all the closed pores have been opened, and the generation of g_2 and tar is finished. Therefore, the increase of the porosity becomes slower. However, a significant number of side chains still remain in the particle at this point, and g_1 continues to be generated as the side chains detach from the aromatic cluster network. The increase of g_1 porosity becomes the main reason for the increase of particle porosity at the later stage of pyrolysis.

3.2. Change of Surface Area during Pyrolysis. The changes in surface area of lignite particles with increasing mass release during pyrolysis calculated by the model are compared to the experimental data in Figure 3. The surface area calculated by the model for the different data sets agrees well with most of the experimental data.

During pyrolysis, the main reason for the increase of S_{particle} is the increasing quantity of the pores that can adsorb adsorbent. Values of $N_{\text{cluster}}^{\text{adsorption pore}}$ and S_{particle} increase with mass release as shown in Figure 4. The increasing trends of $N_{\text{cluster}}^{\text{adsorption pore}}$ and S_{particle} are almost synchronized.



(a) N_2 surface area



(b) CO_2 surface area

Figure 3. Comparison of predicted and measured surface areas of lignite coal particles during pyrolysis.

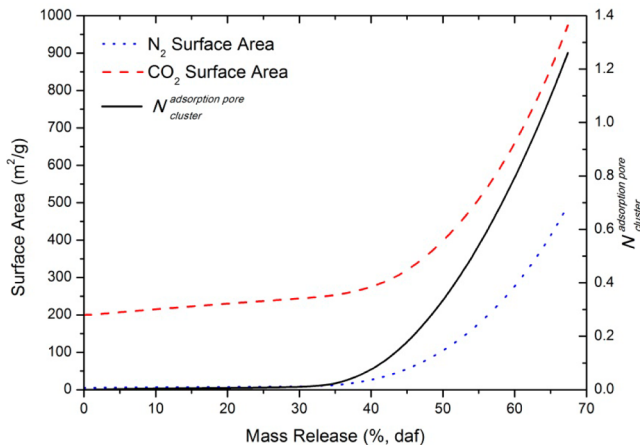


Figure 4. Predicted changes of $N_{\text{cluster}}^{\text{adsorption pore}}$ and S_{particle} with mass release. (Zap lignite).

The change of $N_{\text{cluster}}^{\text{adsorption pore}}$ during pyrolysis is caused by the generation of g_1 . The changes of g_1 , g_2 , and $N_{\text{cluster}}^{\text{adsorption pore}}$ with mass release are shown in Figure 5. At the beginning of

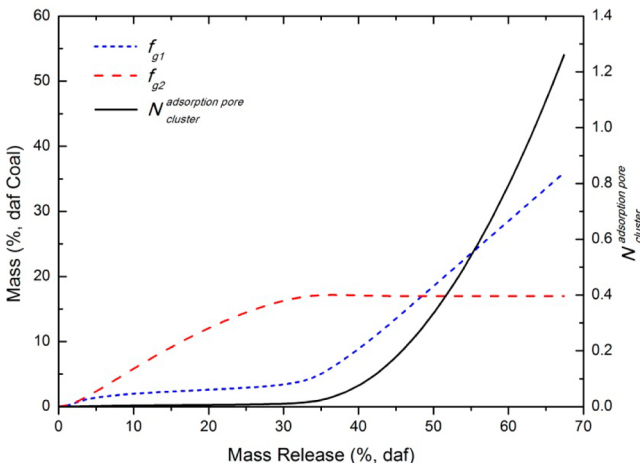


Figure 5. Predicted changes of g_1 , g_2 , and $N_{\text{cluster}}^{\text{adsorption pore}}$ with increasing mass release during pyrolysis (Zap lignite).

pyrolysis, g_2 is generated when a char bridge forms. The space left in the coal macromolecular array when g_2 is released is not big enough to adsorb an adsorbent molecule. The cracking reaction of a bridge to form side chains is almost as fast as the char formation reaction. However, the reaction to form gas from the side chains has a higher activation energy; hence, the yield of g_1 is small at the early stage of pyrolysis. After the mass release is more than 30%, as more side chains are formed in the early stage of the pyrolysis and the temperature increases, g_1 is generated rapidly and the quantity of the adsorption pores is increased.

With the generation of tar, some adsorption sites in pores are removed from the particle and the particle surface area decreases. The changes of the surface area during pyrolysis were examined by comparing two calculation methods: (1) the removal effect of tar to adsorption pores is considered, $N_{\text{clust-coal}} = (1 - A_{\text{ad}})(1/M_{\text{clust}} - N_{\text{clust-tar}})m_p^0$, and (2) the removal effect is ignored, $N_{\text{clust-coal}} = (1 - A_{\text{ad}})/M_{\text{clust}}m_p^0$. The results are compared in Figure 6. The surface area for the case where surface area is decreased because of tar evolution (condition 1)

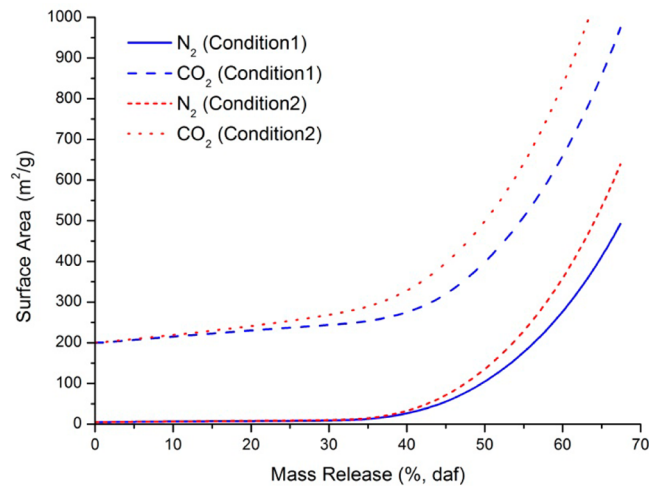


Figure 6. Predicted changes of surface area with mass release during pyrolysis with and without the removal effect of tar (Zap lignite).

is reduced by as much as 25% at a given value of mass release, indicating that the removal effect of tar on adsorption pores is significant.

3.3. Influence of Maximum Particle Temperature. The porosities and surface areas of Zap lignite particle during pyrolysis at various T_{max} are calculated at an ambient pressure of 0.1 MPa. The particles are heated at 1×10^4 K/s from 300 K to various values of T_{max} and then held at that temperature until 600 ms has elapsed.

3.3.1. Porosity. The changes of the porosity of Zap lignite during pyrolysis at various T_{max} are shown in Figure 7. The final

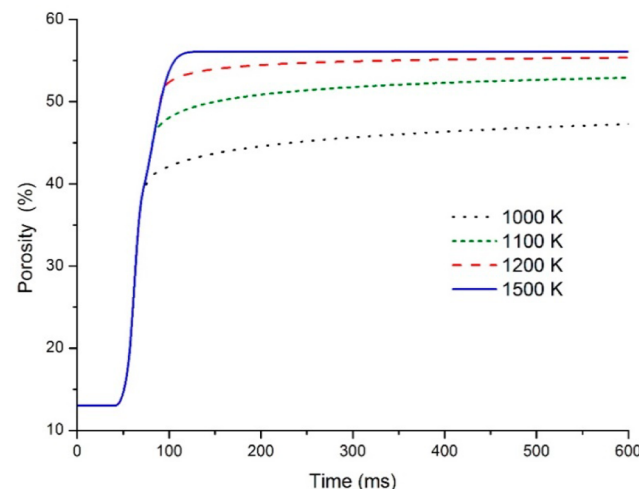


Figure 7. Predicted changes of porosity during pyrolysis at various T_{max} (Zap lignite). Calculations were performed at 0.1 MPa and 1×10^4 K/s, holding at the final temperature until 600 ms elapsed time.

particle porosity increased with increasing T_{max} . A higher temperature can provide more energy for the bridges and side chains cracking to generate more light gases, and a higher temperature can also increase the vaporization of metaplast. Therefore, the space left by the volatiles in the particle is increased with the increase of T_{max} . However, the porosity cannot increase with increasing T_{max} without limit. When T_{max} is high enough (higher than 1200 K) and most of the labile

bridges have been cleaved, the increase of the porosity with further increase of T_{\max} is small (Figure 7).

Because the tar yield of lignite is small, the increase of θ_{tar} with T_{\max} is small, and the dominant factor for the increase of porosity is the increasing θ_{gas} as shown in Figure 8.

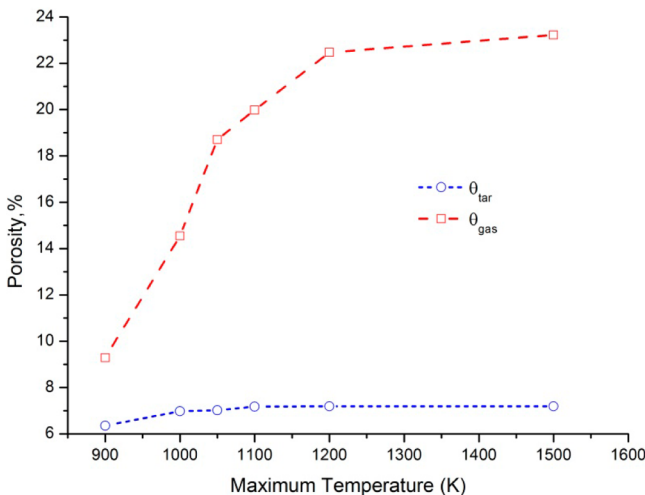


Figure 8. Predicted changes of final θ_{gas} and θ_{tar} during pyrolysis with the increasing T_{\max} . Calculations were performed at 0.1 MPa and 1×10^4 K/s, holding at the final temperature until 600 ms elapsed time.

3.3.2. Surface Area. The changes of the N_2 surface area, the CO_2 surface area, and $N_{\text{cluster}}^{\text{adsorption pore}}$ during pyrolysis of Zap lignite at various T_{\max} are shown in Figure 9. (Note the changes in scale on the y axis.)

The surface area predicted by the model in this paper increases with increasing T_{\max} . The increase in surface area is mainly caused by the larger yield of g_1 at a higher T_{\max} . The g_1 spaces in the particle increased with increasing g_1 yield.

3.3.3. Comparison to the Experimental Data. The predicted change of final porosity and surface area of lignite particle with increasing T_{\max} are compared with experimental results,¹¹ as shown in Figures 10 and 11, respectively. These experimental data are the same as the data from Gale¹¹ that are included Figures 1 and 3 herein (heating rates from 1.0×10^4 to 7.47×10^4 K/s and T_{\max} from 972 to 1625 K) but plotted versus temperature instead of mass release. The calculations are made on the basis of two conditions: (a) The heating rate is constant, 1×10^4 K/s. (b) The temperature histories are the actual temperature histories in the experiment.

The predicted trend of final porosity and surface area of lignite with T_{\max} agrees with the experimentally observed trends in experiments in general, especially at temperatures lower than 1200 K. However, at higher T_{\max} , the model does not match the data.

The difference between the predicted and the experimental results at the maximum temperature of 1330 K in Figure 11 is influenced by the difference in the volatile yield predicted by the CPD model and the data at this temperature (mass release in Figure 11). The predicted results were then adjusted by using the actual experimental volatile yields (cross symbols in Figure 11), which caused the predictions of surface area to agree more closely with the measurements.

The predicted trend of porosity and surface area of lignite particle with increasing mass release generally agrees well with the experimental data (Figures 1 and 3). However, not all the

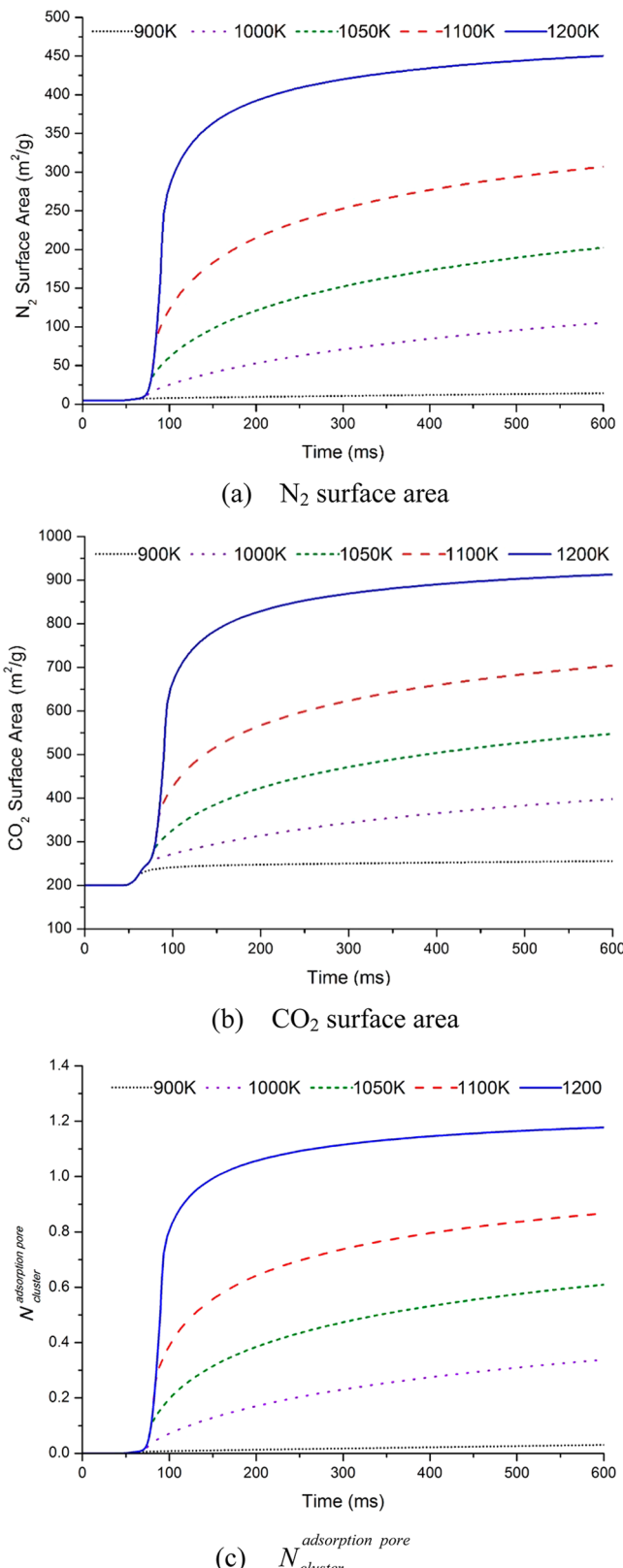


Figure 9. Predicted changes of surface area and $N_{\text{cluster}}^{\text{adsorption pore}}$ during pyrolysis at various values of T_{\max} . Calculations were performed at 0.1 MPa and 1×10^4 K/s, holding at the final temperature until 600 ms elapsed time.

predicted points match the experimental data because the pore structure is influenced by many factors. Although the particle

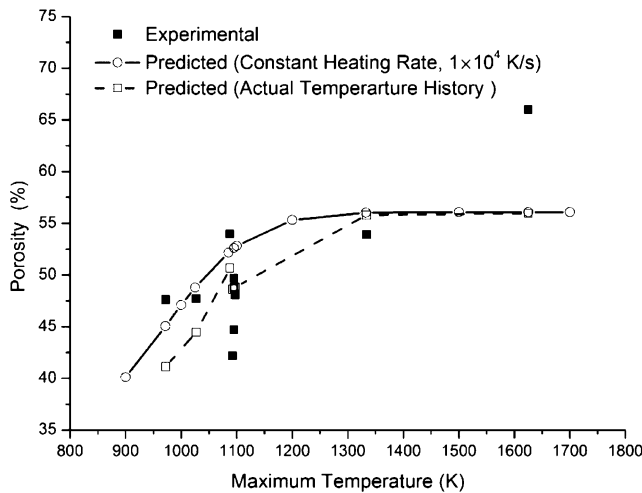


Figure 10. Comparison of the predicted trend of lignite particle porosity during pyrolysis with increase of T_{\max} to experimental data (Zap lignite).¹¹

diameter changes little during pyrolysis, the lignite can also be observed to have melted, bubbled, and swelled at very high heating rate,³⁵ and in addition, the ash in the coal may melt at very high temperatures, which contradicts the “no plastic deformation” assumption in the paper. The porosity larger than 65% observed by the experiment at the temperature higher than 1500 K cannot be obtained by the model in this paper, and the

predicted surface area is much greater than the experimental result at this temperature. The data points at the temperature of 1625 K in Figures 10 and 11 are the points at a mass release of about 60% in Figures 1 and 3, and at the same mass release, the predicted result does not match the experiment. At a temperature of 1625 K, the particle should have been melted. In this condition, many pores are closed by metaplast and melted ash, making the surface area decrease. In contrast, the swelling of bubbles in the particle would make the porosity increased. The model for the pore change at values of T_{\max} higher than 1500 K that consider the melted ash and metaplast is a subject of ongoing research.

3.4. Influence of Heating Rate. The changes of porosity and surface area of a Zap lignite particle during pyrolysis at a T_{\max} of 1000 K, ambient pressure of 0.1 MPa, and various reaction heating rates (constant during pyrolysis) are compared in Figure 12. The total time of the heating process and the hold time at T_{\max} was 560 ms.

At a higher heating rate, the particle can reach a higher temperature more quickly, which can improve the cracking of the aliphatic structure and the vaporization of metaplast. Therefore, the porosity and surface area increase with the increasing heating rates. However, the increases of the porosity and surface area are small. The evolution of pore structure during pyrolysis is determined by the generation of volatiles. The heating rate just determines the time that lignite particle gets to the T_{\max} , but at the same temperature, the reaction rate

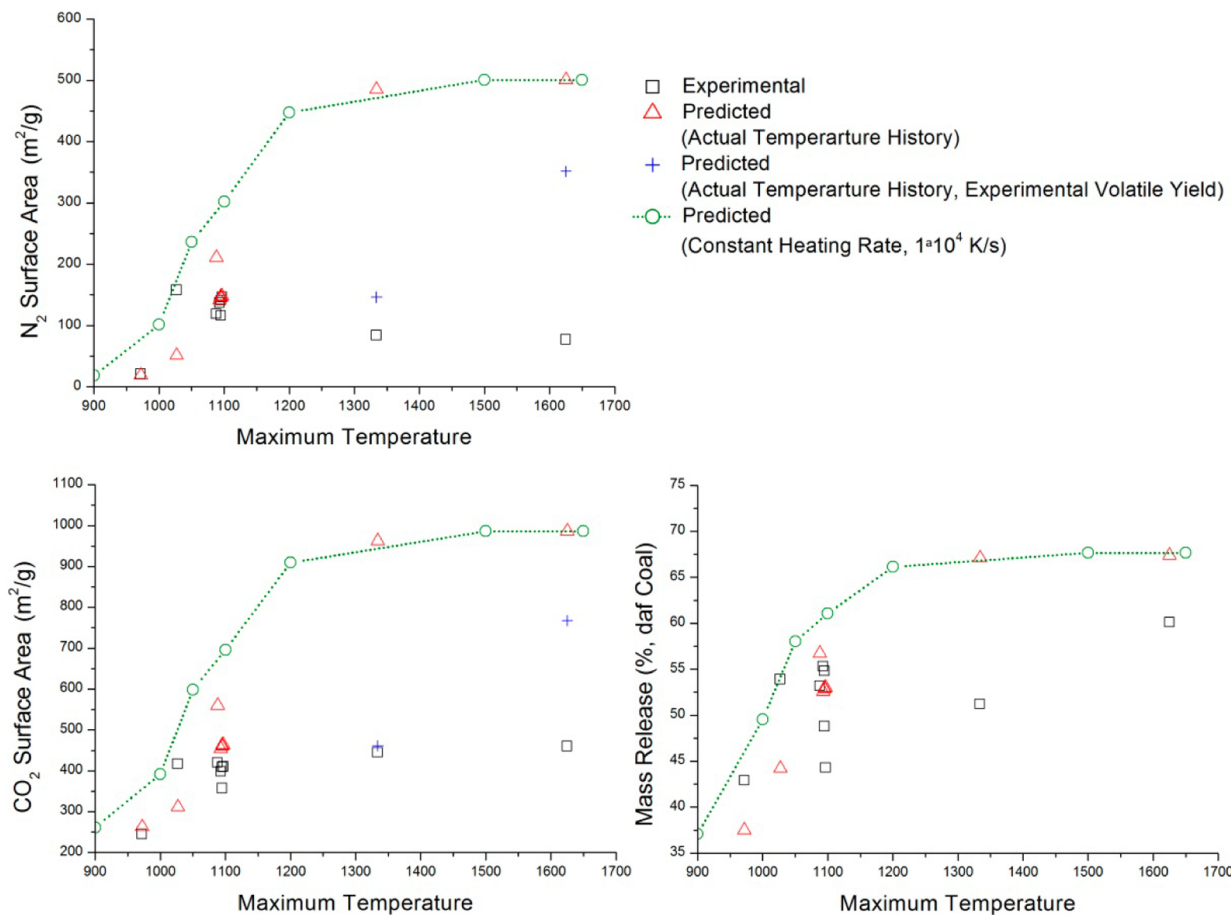


Figure 11. Comparison of the predicted trend of lignite particle surface area during pyrolysis with increase of T_{\max} to experimental data.¹¹

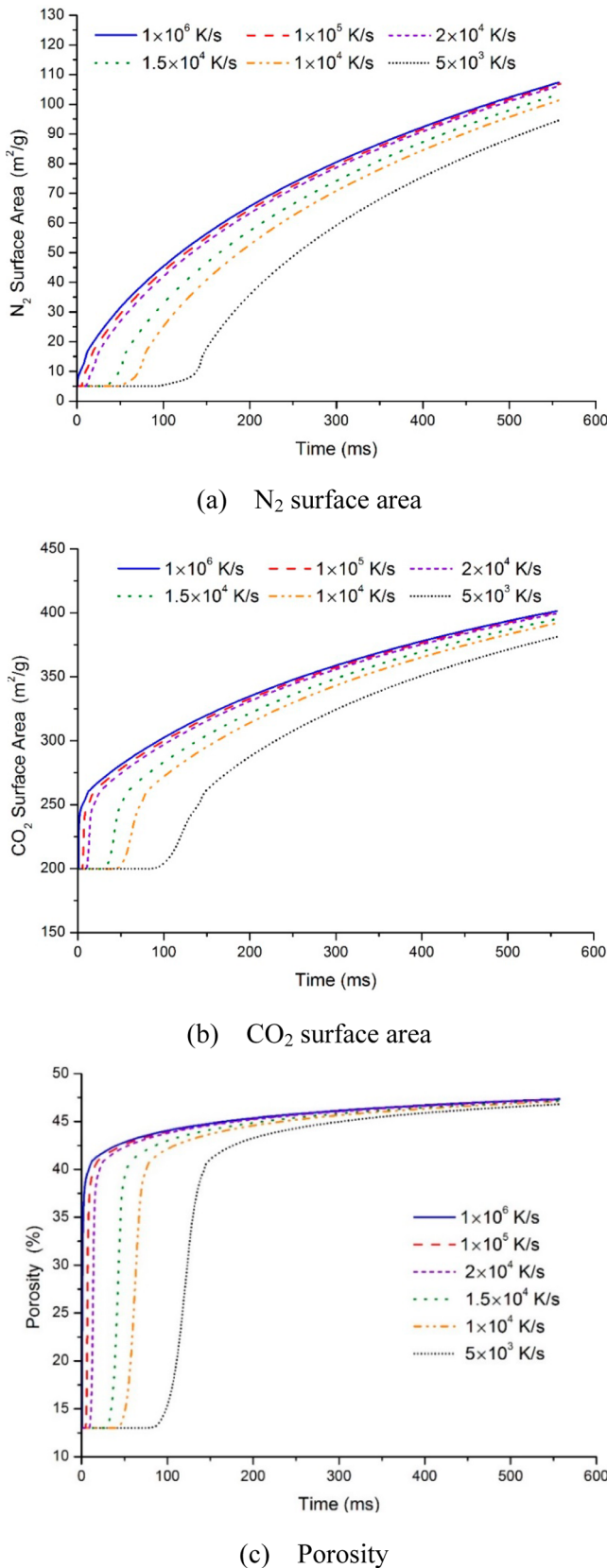


Figure 12. Predicted changes of pore structure during pyrolysis at various heating rates. Calculations were performed at 0.1 MPa and final temperature of 1000 K, holding at the final temperature until 560 ms elapsed time.

is similar. The influence of heating rate on the change of the pore structure of lignite during pyrolysis is therefore limited.

Obvious increasing trends of the porosity and surface area with increasing heating rate were observed in some experiments.¹¹ However, among most experiments, the heating rates were changed by changing the ambient temperature; therefore, the increasing trend may mainly be caused by the increasing T_{max} .

3.5. Influence of Ambient Pressure. The calculated changes of porosity and surface area at a T_{max} of 1000 K, heating rate of 1×10^4 K/s (constant during pyrolysis), and various ambient pressures are compared. The ambient pressure is set as 0.1, 0.2, and 0.3 MPa. Thermoplastic deformation occurred at ambient pressures greater than 0.3 MPa. Under the ambient pressure covered in this paper, the change of tar and gas yield with increasing ambient pressure is small as shown in Figure 13, and the influence of ambient pressure on the change

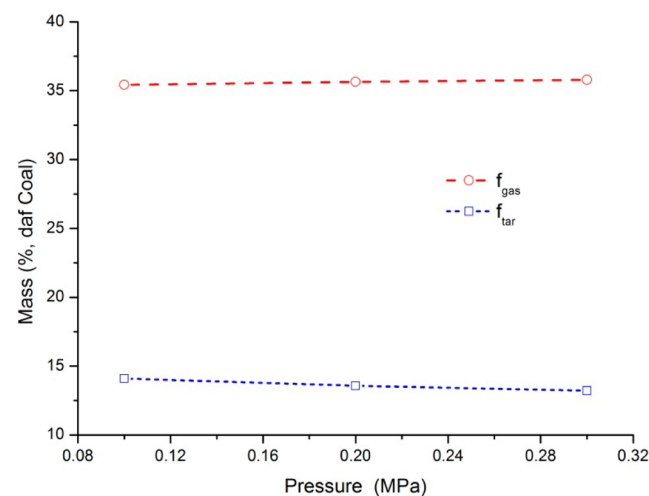


Figure 13. Predicted changes of volatile yield with increasing ambient pressure (Zap lignite). Calculations were performed at 1×10^4 K/s and final temperature of 1000 K, holding at the final temperature until 560 ms elapsed time.

of the pore structure of lignite during pyrolysis is therefore small as shown in Figure 14. Changes in ambient pressure may influence the pore structure significantly at higher pressures, but this model is limited to regimes with no thermoplastic deformation.

In industrial coal combustion processes, maximum particle temperature, heating rate, and ambient pressure influence the pore structure together. High temperature and high ambient pressure both can cause plastic deformation in the particle. During the swelling process, the T_{max} , heating rate, and ambient pressure significantly influence the pore structure, as discussed in previous pyrolysis studies of high-volatile bituminous coal.^{8,21} However, for nonswelling coals as described in this paper, the influences of heating rate and ambient pressure on the pore structure evolution of solid coal during pyrolysis are small.

3.6. Influence of Coal Polymer Structure Parameters. A set of computations were performed to analyze the influence of each coal polymer structure parameter on the change in pore structure during pyrolysis. One polymer structure parameter was changed at a time from the base set of polymer structure parameters for Zap lignite. The heating condition was a T_{max} of 1000 K, a heating rate of 1×10^4 K/s, and an ambient pressure

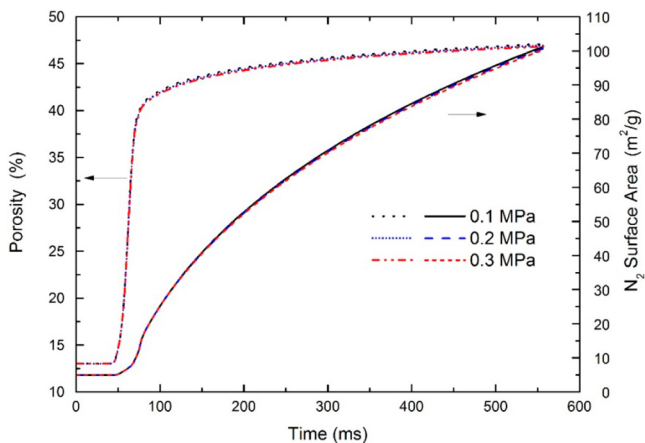


Figure 14. Predicted changes of pore structure parameters during pyrolysis at various external pressures (Zap lignite). Calculations were performed at 1×10^4 K/s and final temperature of 1000 K, holding at the final temperature until 560 ms elapsed time.

of 0.1 MPa. The particle was heated from 300 K to T_{\max} and then held at that temperature until 560 ms had elapsed.

Although the model in this paper is established on the basis of lignite, it theoretically should also be applicable for the solid stage in pyrolysis of swelling coal after considering the influence of the thermal plastic stage. Therefore, to analyze the influence of polymer structure parameters more completely, the range of polymer structure parameters is not limited to lignite in this sensitivity analysis.

3.6.1. Intact Bridges (p_0). A larger p_0 indicates a higher initial quantity of intact bridges in the coal and a smaller initial quantity of side chains. With an increasing quantity of initial intact bridges, the amount of labile aliphatic bridges is increased, which in turn increases the yields of g_2 and the char bridges. Meanwhile, the yield of g_1 is decreased with the decreasing initial quantity of side chains. Because the reaction generating g_2 is faster and more easily occurs at a lower temperature, the labile aliphatic bridges in the g_2 generation reaction can be transformed more completely than the side chains in the g_1 generation reaction. The increase of g_2 yield is therefore larger than the decline of the g_1 yield as shown in Figure 15, and the total yield of the light gases is increased, making θ_{gas} increase with increasing p_0 . With the increasing generation of the char bridges, more aromatic clusters can be bonded to the coal matrix, which in turn decreases the tar yield, and θ_{tar} is therefore decreased with the increasing p_0 . Because the increase of θ_{gas} is smaller than the decrease of θ_{tar} , the total porosity θ is decreased with increasing p_0 as shown in Figure 16.

The decreased tar yield decreases the quantity of g_1 spaces removed by the tar from the coal particle during pyrolysis. However, the decreasing initial quantity of side chains can decrease the generation of g_1 spaces directly. Therefore, surface area of the char particle increases and then decreases with increasing p_0 as shown in Figure 17.

3.6.2. Initial Char Bridges (c_0). The increasing c_0 decreases the yield of tar (Figure 18), and θ_{tar} is therefore decreased (Figure 19). The decreased tar yield means more aliphatic structures remain in the particle, along with the associated number of side chains, which in turn increases the yield of gas (Figure 18). Therefore, θ_{gas} is increased (Figure 19), and the surface area increases as shown in Figure 25. The increased

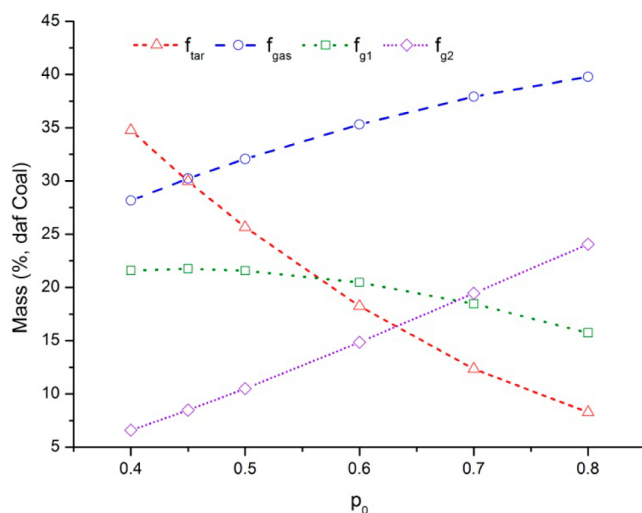


Figure 15. Change of the predicted volatile yield with increasing p_0 .

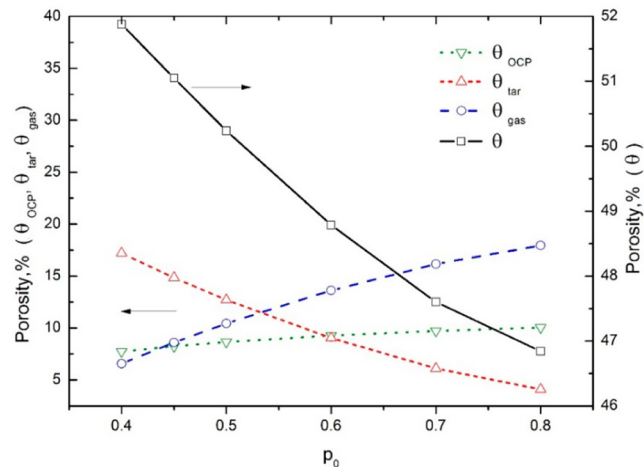


Figure 16. Change of the predicted char porosity with increasing p_0 .

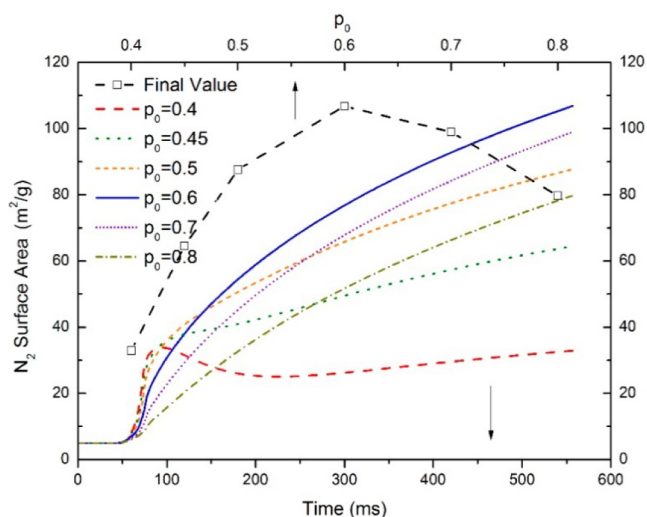


Figure 17. Change of the predicted char surface area with increasing p_0 .

initial quantity of unbreakable bridges makes more closed pores that cannot be opened, causing decreased θ_{OCP} (Figure 19). Because the increase of θ_{gas} is smaller than the decrease of θ_{tar}

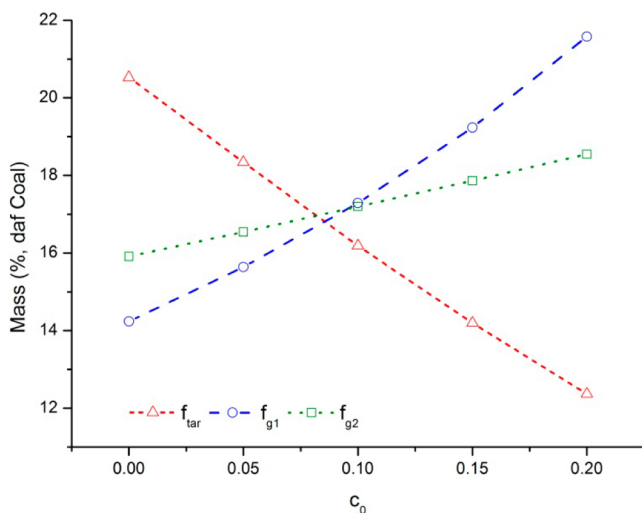


Figure 18. Change of the predicted volatile yield with increasing c_0 .

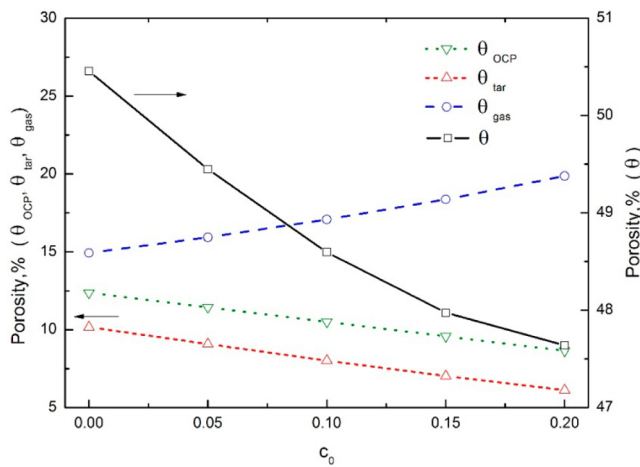


Figure 19. Change of the predicted char porosity with increasing c_0 .

and θ_{OCP} , the total porosity θ is decreased with increasing c_0 as shown in Figure 20.

3.6.3. Coordination Number ($\sigma+1$). A larger value of $\sigma+1$ indicates that there are more aliphatic structures (bridges and

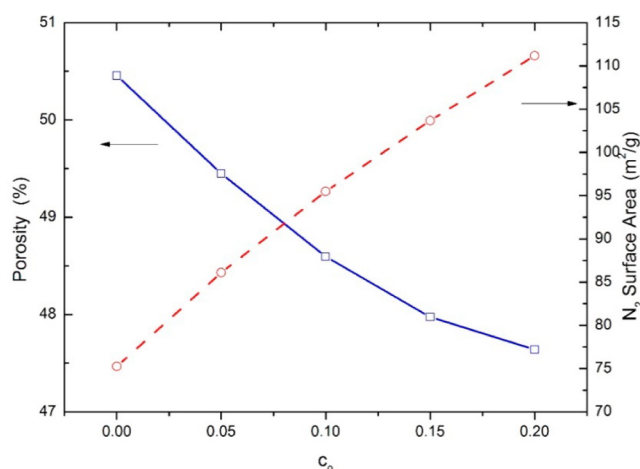


Figure 20. Change of the predicted char pore structure parameters with increasing c_0 .

side chains) on each cluster and that the coal is more cross-linked initially. The yield of light gases (both g_1 and g_2), which are generated from the aliphatic structures, is therefore increased (Figure 21) with increasing $\sigma+1$, making θ_{gas} increase

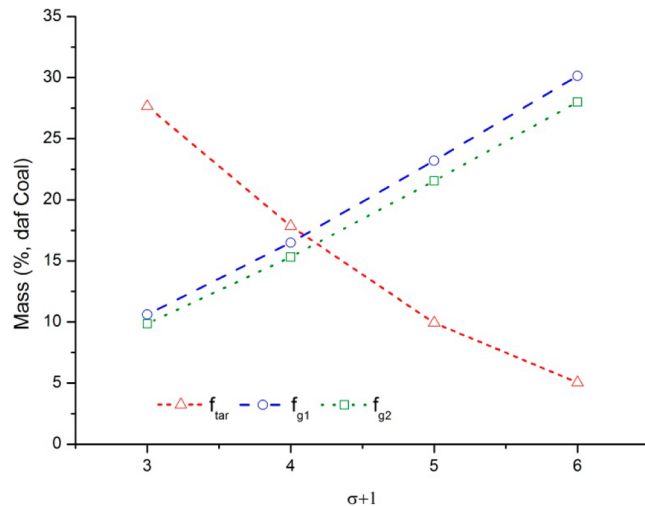


Figure 21. Change of the predicted volatile yield with increasing $\sigma+1$.

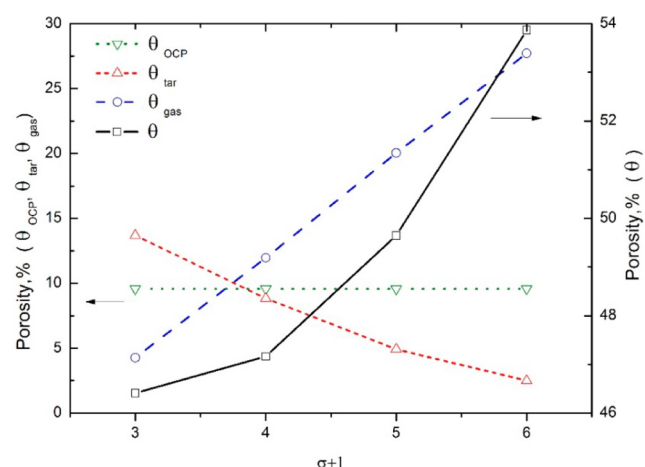


Figure 22. Change of the predicted char porosity with increasing $\sigma+1$.

as shown in Figure 22. However, because a larger quantity of bridges can provide more connection between each aromatic cluster and coal matrix, the probability for each aromatic cluster to be detached from the coal matrix is decreased, which in turn decreases the yield of tar (Figure 21) and makes θ_{tar} decrease (Figure 22). The decrease of θ_{tar} is smaller than the increase of θ_{gas} and θ is therefore increased with increasing $\sigma+1$ as shown in Figure 22.

In addition, because the quantity of g_1 spaces in the coal is increased with the increasing yield of g_1 and the decreasing yield of tar, the particle surface area is increased with the increasing $\sigma+1$ as shown in Figure 23.

3.6.4. M_{clust} and M_δ . The values of M_{clust} and M_δ determine the mass (and hence volume) proportions of aromatic clusters and bridges in the coal polymer network. With increasing M_{clust} , the proportions of aromatic clusters are increased, and the proportions of the bridges are decreased. The final char formed

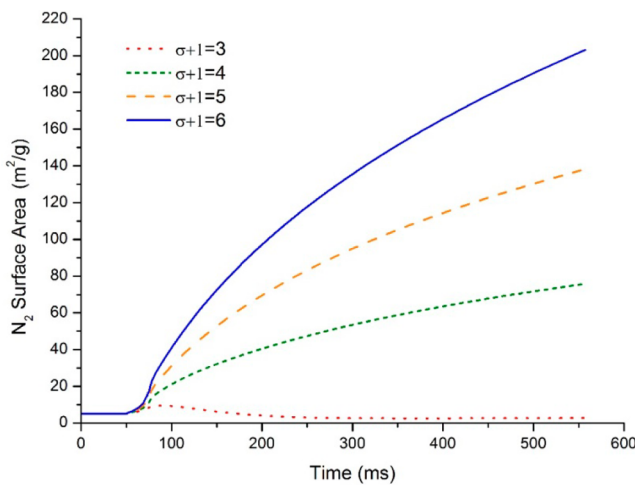


Figure 23. Predicted change of the surface area during pyrolysis under various $\sigma+1$.

during pyrolysis consists of many aromatic clusters (without the labile aliphatic attachments) connected by char bridges. With the increase of M_{clust} , the mass remained in the char is increased, and the specific surface area is therefore decreased as shown in Figure 24. Meanwhile, in the final char, because the

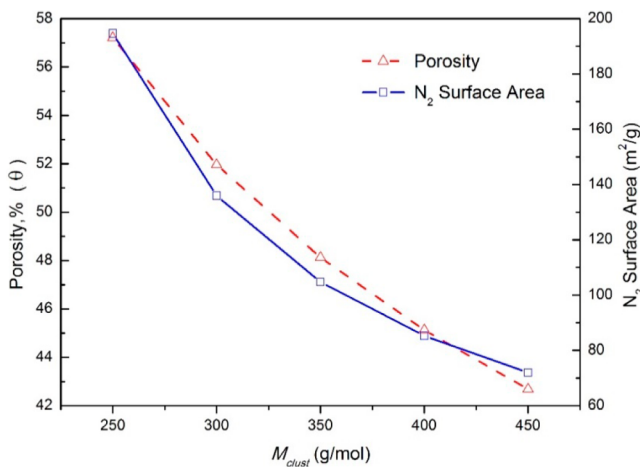


Figure 24. Predicted changes of porosity and surface area with increasing M_{clust} .

volume proportion of g_1 spaces and g_2 spaces is decreased with the decreasing volume proportion of the bridges in the initial coal, the porosity of the char is decreased with increasing M_{clust} as shown in Figure 24. In contrast, the porosity and surface area of the char increase with increasing M_δ as shown in Figure 25.

4. CONCLUSIONS

In this paper, using the coal polymer network parameters in the CPD model to calculate the particle surface area and porosity, a model for the evolution of pore structure in a lignite particle during pyrolysis is established. The calculation results match the porosity and surfaces area of the lignite particle during pyrolysis measured in the experiments at temperatures lower than 1200 K. The rapid increase of surface area when the mass release reaches 30% was explained by the change in the quantity of pores that can adsorb adsorbent in the particle during pyrolysis because of the cracking of side chains.

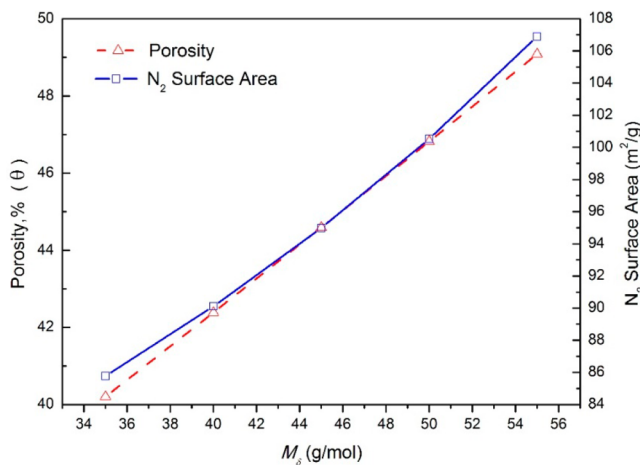


Figure 25. Predicted changes of porosity and surface area with increasing M_δ .

However, the model agreement with surface area data becomes poorer at temperatures above 1200 K, which may be due to potential softening or melting of the char or ash.

When the mass release is less than 30%, the increase of the predicted porosity is caused by the opening of the closed pores and the increasing volume of the spaces left by the volatile in the particle. When the mass release is greater than 30%, the increase of the predicted porosity is mainly caused by increasing volume of the spaces left by cracked side chains in the particle.

The predicted porosity and surface area of char formed from lignite during pyrolysis increase with increasing T_{max} because a higher temperature can make the side chains and bridges crack more completely with subsequent formation of more micro-pores. The influence of heating rate and ambient pressure on the pore structure of lignite during pyrolysis is small.

The predicted porosity of the char increases with increasing $\sigma+1$ and M_δ and decreases with increasing p_0 , c_0 , and M_{clust} . The predicted surface area increases with increasing c_0 , $\sigma+1$, and M_δ , decreases with increasing M_{clust} , and first increased and then decreased with the increasing p_0 .

■ AUTHOR INFORMATION

Corresponding Author

*E-mail: lisuf@dlut.edu.cn.

Notes

The authors declare no competing financial interest.

■ ACKNOWLEDGMENTS

This work is supported in part by a scholarship from the China Scholarship Council (CSC) under the grant CSC no. 201306060059 and performed at Brigham Young University while H.Y. was a visiting graduate student.

■ REFERENCES

- (1) Bayless, D. J.; Schroeder, A. R.; Peters, J. E.; Buckius, R. O. Effects of surface voids on burning rate measurements of pulverized coal at diffusion-limited conditions. *Combust. Flame* 1997, 108, 187–198.
- (2) Zeng, D.; Clark, M.; Gunderson, T.; Hecker, W. C.; Fletcher, T. H. Swelling properties and intrinsic reactivities of coal chars produced at elevated pressures and high heating rates. *Proc. Combust. Inst.* 2005, 30, 2213–2221.

- (3) Bailey, J. G.; Tate, A.; Diessel, C. F. K.; Wall, T. F. A char morphology system with applications to coal combustion. *Fuel* **1990**, *69*, 225–239.
- (4) Zygourakis, K. Effect of pyrolysis conditions on the macropore structure of coal derived chars. *Energy Fuels* **1993**, *7* (1), 33–41.
- (5) Sheng, S.; Azevedo, J. L. T. Modeling the evolution of particle morphology during coal devolatilization. *Proc. Combust. Inst.* **2000**, *28*, 2225–2232.
- (6) Yu, J.; Lucas, J.; Wall, T.; et al. Modeling the development of char structure during the rapid heating of pulverized coal. *Combust. Flame* **2004**, *136*, 519–532.
- (7) Oh, M. S.; Peters, W. A.; Howard, J. B. An experimental and modeling study of softening coal pyrolysis. *AIChE J.* **1989**, *35* (5), 775–792.
- (8) Yang, H.; Li, S.; Fletcher, T. H.; Dong, M. Simulation of the swelling of high-volatile bituminous coal during pyrolysis. *Energy Fuels* **2014**, *28* (11), 7216–7226.
- (9) Fletcher, T. H.; Hardesty, D. R. *Compilation of Sandia Coal Devolatilization Data: Milestone Report*; report no. SAND92-8209 prepared for Sandia National Laboratories: Livermore, CA, USA, 1992; pp 5–43.
- (10) Wang, X.; Li, S.; Zhao, Q. Specific area and pore structure evolution during lignite fast pyrolysis. *Coal Conversion* **2013**, *36* (4), 6–9, 89.
- (11) Gale, T. K.; Fletcher, T. H.; Bartholomew, C. H. Effects of pyrolysis conditions on internal surface areas and densities of coal chars prepared at high heating rates in reactive and non-reactive atmospheres. *Energy Fuels* **1995**, *9*, 513–524.
- (12) Nsakala, N. Y.; Essenhigh, R. H.; Walker, P. L. Characteristics of chars produced from lignites by pyrolysis at 808°C following rapid heating. *Fuel* **1978**, *57*, 605–611.
- (13) Yang, H.; Li, S.; Fletcher, T. H.; Dong, M. Simulation of the Swelling of High Volatile Bituminous Coal during Pyrolysis: 2. Influence of Maximum Particle Temperature. *Energy Fuels* **2015**, *29* (6), 3953–3962.
- (14) Hu, Z.; Xie, G.; Guo, Z.; Wang, Q.; Fang, M.; Luo, Z.; Cen, K. Effects of pyrolysis temperature on pore structure and combustion characteristics of high-moisture Indonesia lignite semi-coke. *Therm. Power Gener. (Xi'an, China)* **2014**, *43* (10), 74–78.
- (15) Yang, X.; Zhang, C.; Tan, P.; Yang, T.; Fang, Q.; Chen, G. Properties of Upgraded Shengli Lignite and Its Behavior for Gasification. *Energy Fuels* **2014**, *28* (1), 264–274.
- (16) Xu, S.; Zhou, Z.; Yu, G.; Wang, F. Effects of Pyrolysis on the Pore Structure of Four Chinese Coals. *Energy Fuels* **2010**, *24*, 1114–1123.
- (17) Liu, T.-f.; Fang, Y.-t.; Wang, Y. Rapid pyrolysis of coal at high temperature. *J. Fuel Chem. Technol. (Beijing, China)* **2009**, *37* (1), 20–25.
- (18) Zhu, X.; Sheng, C. Evolution of the Char Structure of Lignite under Heat Treatment and Its Influences on Combustion Reactivity. *Energy Fuels* **2010**, *24*, 152–159.
- (19) Chen, L.; Zhou, Z.; Liu, X.; Yuan, S.; Wang, F. Effect of microstructure of rapid pyrolysis char on its gasification reactivity. *J. Fuel Chem. Technol. (Beijing, China)* **2012**, *40* (6), 648–654.
- (20) Yu, Y.; Xu, M.; Yu, D.; Huang, J. Fragmentation of coal particles by devolatilization during combustion. *J. Huazhong Univ. Sci. Technol., Nat. Sci.* **2005**, No. 8, 8–11.
- (21) Yang, H.; Li, S.; Fletcher, T. H.; Dong, M.; Zhou, W. Simulation of the evolution of pressure in a lignite particle during pyrolysis. *Energy Fuels* **2014**, *28* (5), 3511–3518.
- (22) Solomon, P. R.; Hamblen, D. G.; Yu, Z. Z.; Serio, M. A. Network models of coal thermal-decomposition. *Fuel* **1990**, *69* (6), 754–763.
- (23) Shurtz, R. C.; Hogge, J. W.; Fowers, K. C.; Sorensen, G. S.; Fletcher, T. H. Coal swelling model for pressurized high particle heating rate pyrolysis applications. *Energy Fuels* **2012**, *26*, 3612–3627.
- (24) Shurtz, R. C.; Kolste, K. K.; Fletcher, T. H. Coal swelling model for high heating rate pyrolysis applications. *Energy Fuels* **2011**, *25*, 2163–2173.
- (25) Fletcher, T. H. Time-resolved temperature-measurements of individual coal particles during devolatilization. *Combust. Sci. Technol.* **1989**, *63* (1–3), 89–105.
- (26) Serio, M. A.; Hamblen, D. G.; Markham, J. R.; Solomon, P. R. Kinetics of volatile product evolution in coal pyrolysis: experiment and theory. *Energy Fuels* **1987**, *1* (2), 138–152.
- (27) Solomon, P. R.; Hamblen, D. G.; Carangelo, R. M.; Serio, M. A.; Deshpande, G. V. General model of coal devolatilization. *Energy Fuels* **1988**, *2*, 405–422.
- (28) Niksa, S.; Kerstein, A. R. FLASHCHAIN theory for rapid coal devolatilization kinetics. 1. Formulation. *Energy Fuels* **1991**, *5* (5), 647–665.
- (29) Niksa, S. FLASHCHAIN theory for rapid coal devolatilization kinetics. 3. Modeling the behavior of various coals. *Energy Fuels* **1991**, *5* (5), 673–683.
- (30) Niksa, S. FLASHCHAIN theory for rapid coal devolatilization kinetics. 2. Impact of operating-conditions. *Energy Fuels* **1991**, *5* (5), 665–673.
- (31) Fletcher, T. H.; Kerstein, A. R.; Pugmire, R. J.; Solum, M. S.; Grant, D. M. Chemical percolation model for devolatilization. 3. Direct Use of ¹³C NMR Data to Predict Effects of Coal Type. *Energy Fuels* **1992**, *6* (4), 414–431.
- (32) Fletcher, T. H.; Kerstein, A. R.; Pugmire, R. J.; Grant, D. M. Chemical percolation model for devolatilization. 2. Temperature and heating rate effects on product yields. *Energy Fuels* **1990**, *4*, 54–60.
- (33) Grant, D. M.; Pugmire, R. J.; Fletcher, T. H.; Kerstein, A. R. Chemical model of coal devolatilization using percolation lattice statistics. *Energy Fuels* **1989**, *3*, 175–186.
- (34) Genetti, D. B. *An advanced model of coal devolatilization based on chemical structure*. M.S. Thesis, Brigham Young University, Provo, UT, 1999.
- (35) Gale, T. K. *Effects of pyrolysis condition on coal char properties*. Ph.D. Dissertation, Brigham Young University, Provo, 1994.